ROOM
-VENT
'90

Computation of conduction, convection and radiation in the perimeter zone of an office space

A2

M.J. Holmes
J. K-W. Lam
K.G. Ruddick
G.E. Whittle
Arup Research and Development
London, UK

COMPUTATION OF CONDUCTION, CONVECTION AND RADIATION IN THE PERIMETER ZONE OF AN OFFICE SPACE

M.J.Holmes, J.K-W.Lam, K.G.Ruddick, G.E.Whittle
Arup Research and Development
13 Fitzroy Street
London, W1P 6BQ
U.K.

SUMMARY

To ensure a good quality thermal environment it may be necessary in HVAC design to carry out a detailed evaluation of environmental performance using simulation techniques. The tools used are generally the dynamic thermal model and the computational fluid dynamics (CFD) code. These tools are complementary, and this paper describes a study involving a full transient coupling of two such codes (R2D2 and AIRFLO). A test problem consisting of a West-facing perimeter office space with a ceiling-mounted diffuser was considered, and results are presented of simulation over a two hour period on a cold morning. Comparison has been made between full transient coupling and a sequential operation of the codes. The operation of the codes in coupled form highlighted a transient oscillatory behaviour of the air movement field resulting from the nature of the system and controller. The computational overhead of operating the dynamic thermal model was found to be 0.5%. The run-time being dominated by the heavy computational requirements of the transient CFD analysis.

COMPUTATION OF CONDUCTION, CONVECTION AND RADIATION IN THE PERIMETER ZONE OF AN OFFICE SPACE

M.J.Holmes, J.K-W.Lam, K.G.Ruddick, G.E.Whittle
Arup Research and Development
13 Fitzroy Street
London, W1P 6BQ
U.K.

1. INTRODUCTION

The combination of large areas of glazing and a ceiling mounted room air distribution system can, in winter, lead to poor levels of thermal comfort and ventilation effectiveness. This is particularly the case where, due to the need to maximise lettable floor area, under-sill heating may not be acceptable. Under these circumstances the risk of high radiant temperature asymmetry and cold downdraught from the glazing is significant.

Where a good quality thermal environment is vital it is often wise to predict the resulting conditions before finalising the design. This requires a consideration of a number of interacting heat transfer mechanisms including conduction and transmission through the fabric, the radiant exchanges between surfaces, the operation and control of the air conditioning plant and the convection processes occurring within the room.

The interactions between the mechanisms of heat transfer depend on boundary conditions which are also a function of time. The need, therefore, is to be able to represent the important heat transfer processes (and plant control actions) with sufficient flexibility so that all the relevant parameters can be modelled. This may be achieved by using a dynamic thermal model to compute both the transient heat flux through the fabric and the combined heat exchange at surfaces and, hence, to predict the internal surface temperatures. A computational fluid dynamics (CFD) code may then be used to predict the resulting air movement and temperature distribution in the space and the convection processes at surfaces.

Usually, if a detailed analysis involving thermal and air movement modelling is required then it is done by operating a thermal model to provide boundary conditions for the CFD code. In reality, of course, the physical interaction between the mechanisms of heat transfer means that the approach of using the two models should be iterative, with the CFD code, in turn, providing data on temperature distribution and surface convection for the thermal model to work with (1). However, because of the potential complexity of this approach the true iterative nature of this interaction is rarely represented.

In practice, because of the dramatically different timescales (2) it is not known whether the fully integrated approach to modelling the thermal environment is really necessary or, if the need is to focus on air movement, whether a serial use of models is permissible.

In this paper the approach is to directly combine the capabilities of

the dynamic thermal model with those of the CFD code so that the interactions outlined above and their implications can be studied. This is achieved by incorporating algorithms describing fabric conduction and transmission, and surface-to-surface radiant heat transfer into an existing CFD code, and operating the resulting model in transient mode. The model is then applied to simulate a perimeter office space in winter. The influence of the resulting radiant heat transfer and cold downdraught on thermal comfort is studied, comments on the value of integrating the thermal model are made, and the computational overhead of solving the additional equations representing conduction and radiant heat transfer are identified.

2. MODELLING APPROACH

The need to address the issue of simultaneous calculation of heat conduction and radiation for the fabric, air movement in the space and the operation of a thermostatically controlled warm air supply requires a close integration of the simulation software. This has been achieved by drawing on software modules which had already been developed at Arup R&D, but which form the basis of hitherto totally separate programs.

Routines which describe heat conduction through the fabric and surface-to-surface radiation were taken from the Arup R&D dynamic thermal model, ROOM, designated R2D2 (ROOM version 2, dimensions 2) for this study. These were integrated into the Arup R&D CFD code AIRFLO together with additional algorithms describing the air supply controller.

2.1 Dynamic thermal model

The thermal model selected for this exercise is a two dimensional version of a general model (ROOM) developed by Arup R&D. The (two dimensional) model has the following characteristics:

- Explicit finite difference algorithm. Long wave radiant interchange by means of a linearized radiosity model (3).
- Transmitted, direct short wave radiation is distributed onto surface elements according to solar and element priorities.
- All shortwave reflections are non-specular, and dealt with via the radiosity concept using short wave absorption coefficients.
- A single pane of glass has two nodes - one at each surface, solar radiation is absorbed at the nodes and the thermal capacity of the glass is also located there - so glass is modelled as a 2 node network with heat input at both nodes.

The basic algorithm for R2D2, after reading in all data, is:

i) Calculate radiation form factors.

ii) Set up and invert long wave radiosity matrix (Choleski factorization is used in double precision).

iii) Set up and invert short wave radiosity matrix.

iv) Assume an initial internal air temperature and calculate heat transfer temperatures (radiant flows via radiosities) for each surface element.

v) Calculate the model temperatures within all fabric elements using the basic forward-difference equation:

vi) Obtain surface temperatures and hence air temperatures, either:

(A) - assuming a fully mixed space, or

(B) - by transferring surface temperatures to the airflow model.

vii) Calculate transmitted and absorbed solar radiation, and the internal distribution of radiation, then return to iv) using the new air temperature instead of the assumed value.

Typical time steps for the analysis are 30 seconds, the limit being the time constant of the single glazing. For consistency each opaque surface element is set up to have a time constant roughly equal to that of half a pane of 6mm single glazing. This capacity is located at the surface to ensure a very low Biot number.

When assuming a fully mixed space, the convective heat transfer coefficient was taken as $2.5 W/m^2/°C$.

2.1.1 Radiation Form Factors

The simple geometry chosen for this example enables the use of analytical form factors for radiation interchange between surface elements. All values can be obtained from factors for two basic geometries:

(a) Two infinitely long parallel planes of width w displaced by a distance z.

$$F_{1,2} = ((w^2+z^2)^{0.5} - w) / z$$

(b) Two infinitely long planes at right angles; plane 1 is of width z, plane 2 is of width y.

$$F_{1,2} = (1 + y/z - (y^2+z^2)^{0.5}/z) / 2$$

The law of reciprocity and form factor algebra are all that is necessary to obtain values of $F_{m,n}$ for each element of the two-dimensional space.

2.1.2 Treatment of Solar Radiation

Radiation values are read from meteorological office recordings and converted into direct radiation normal to the external wall, and diffuse radiation. Transmitted and absorbed radiation are evaluated theoretically using optical theory. The sol-air temperature is used as the external heat transfer temperature for the external wall. This is calculated with a longwave radiation loss of 1/4 of that for an horizontal surface. This loss is also used in the calculation of glazing temperatures.

The internal distribution of solar radiation is trivial. Simple trigonometry gives the size and location of the daylit areas. Knowing the intensity of the transmitted radiation and angle of incidence between the receiving surface and the sun it is a simple matter to determine the intensity on that surface. In general the daylit area will not cover whole cells, in which case the solar energy is averaged over the part-lit cells.

The most appropriate way to distribute diffuse radiation is more difficult to specify. Levels of diffuse depend upon the source - ground, sky, adjacent buildings, etc. So different intensities can be expected on each room surface. This is ignored, and the pragmatic decision to distribute the diffuse radiation in direct proportion to the radiation form factors between window and room element is taken. Further, all radiation is taken as diffuse on reflection from the room surfaces.

2.2 Air movement model

The computational fluid dynamics code, AIRFLO, has been used for HVAC design at Arup R&D. The code is an implicit integration finite-volume Navier-Stokes solver, which has been developed particularly for application to natural and forced convection air flow problems in buildings.

The code uses a pressure-coupled formulation involving the simultaneous solution of the momentum equations for velocity components, and the mass continuity equation for pressure. The equation for pressure is derived by substituting the momentum equations (for velocity components) into the statement of mass continuity (4). A re-arrangement of terms results in a diagonally-dominant equation for pressure. The mass continuity equation is, therefore, exact thus obviating the need for a pressure-correction algorithm such as SIMPLE or its derivatives (5).

The velocity components are calculated at cell faces using a staggered grid. A standard linearization of the equations is used, where the linearized coefficients comprise the convection and diffusion fluxes over the staggered momentum cells and the scalar temperature cells, as appropriate.

In the work reported here the energy equation is solved in a segregated form where the act of linearization de-couples it from the momentum and mass continuity equations. Although very simple to implement, this can result in the need for substantial under-relaxation to retain stability, and hence the well-known difficulties of delayed convergence in high Rayleigh number buoyant flows. Although not implemented here, a Newton-Raphson linearization of the energy equation would be expected to significantly enhance the convergence rate for buoyant flow (6). Buoyancy force is modelled using the Boussinesq approximation.

The 'hybrid' differencing scheme (5) is used, giving central differences at low Peclet number and upwind differences (with diffusion suppressed) for high Peclet number. A point Gauss-Seidel solver is implemented for all the equations. Appendix A shows the finite-volume form of the equations. In this work the equations are solved in their transient form, where a simple Euler integration with forward differencing in time is used.

Convection at surfaces was modelled by applying data from the CIBSE guide (7). These data define convective heat transfer coefficient as a

function of local air speed, the difference between local air temperature and surface temperature and the orientation of the surface (see Table 1). Linear interpolation was performed on the data. The local air temperature was taken as that at a distance of 100mm from the surface.

Table 1. Convective heat transfer coefficient

Temperature difference (°C)	Air speed (m/s)	Convective heat transfer coefficient ($W/m^2/°C$) Vertical	Horiz.(stable*)	Horiz.(unstable**)
	0.0	1.40	0.64	1.70
	0.1	1.48	0.68	1.80
1	0.3	1.65	0.76	2.00
	0.5	1.82	0.83	2.21
	0.0	2.01	0.84	2.44
	0.1	2.13	0.89	2.59
3	0.3	2.37	0.99	2.88
	0.5	2.62	1.10	3.18
	0.0	2.38	0.96	2.89
	0.1	2.52	1.01	3.07
5	0.3	2.81	1.13	3.41
	0.5	3.10	1.24	3.76

* Hot surface facing down / Cold surface facing up
** Hot surface facing up / Cold surface facing down

3. TEST PROBLEM

3.1 Room and air conditioning system

A 2D slice of a typical perimeter office space is considered. Figure 1 shows the geometry. The room is 2.75m high and 4.9m long with a single-glazed window of height 1.5m set in the external wall, 0.92m from the floor. The office is West-facing.

Heat transfer through internal walls to rooms that are not analyzed is accounted for by assuming that the floor is above a ceiling identical to that in the room under investigation (i.e. cyclic condition), and that conditions are the same either side of the rear wall (i.e. symmetric condition).

The floor/ceiling consists of a carpet, concrete slab and plasterboard ceiling, the front wall is constructed of plasterboard, insulation and brick (overall U-value= $0.4W/m^2/°C$), and the internal wall is a partition of two sheets of plasterboard. The window is single-glazed with 6mm clear glass. Table 2 shows the absorption coefficients of these materials.

For R2D2 the geometry was divided into surface elements (13 for the floor/ceiling and 7 for the walls) each of which covered a number of AIRFLO cell faces. Each element was then represented by a number of nodes (14 for the floor, 6 for the rear wall, 15 for the front wall, 2 for the glass) to give the temperature profile at different thicknesses within the fabric. In

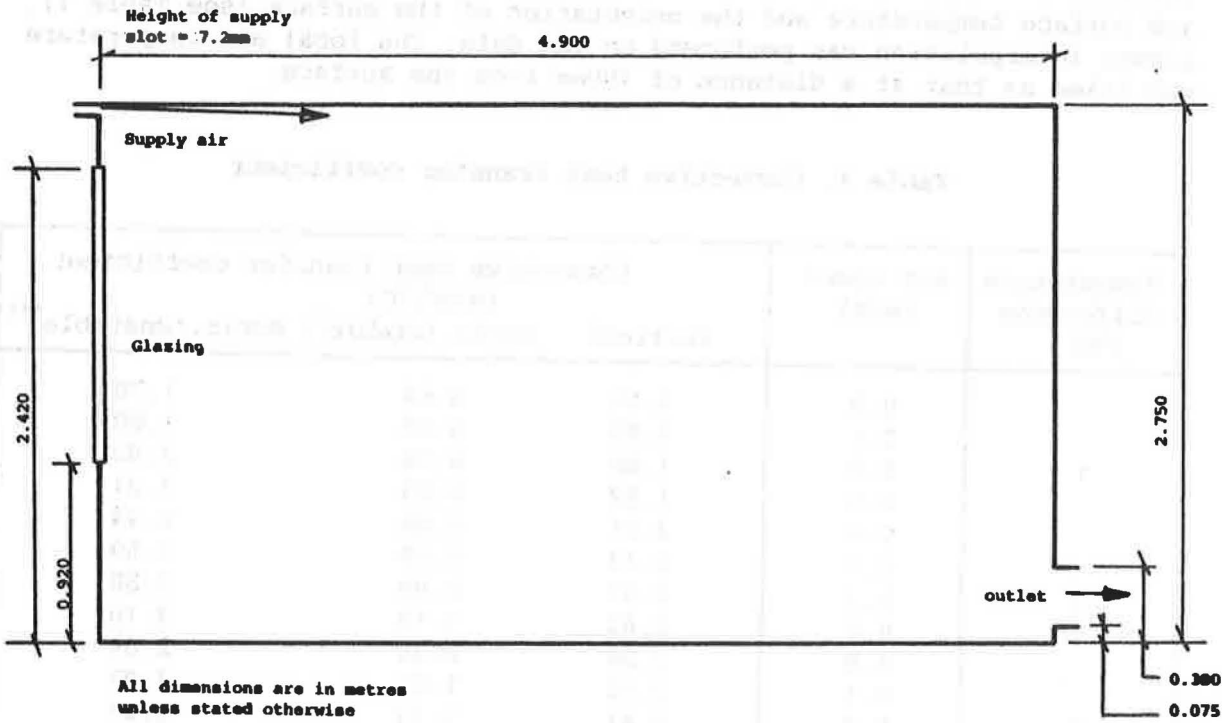

Fig. 1. Cross-section of room.

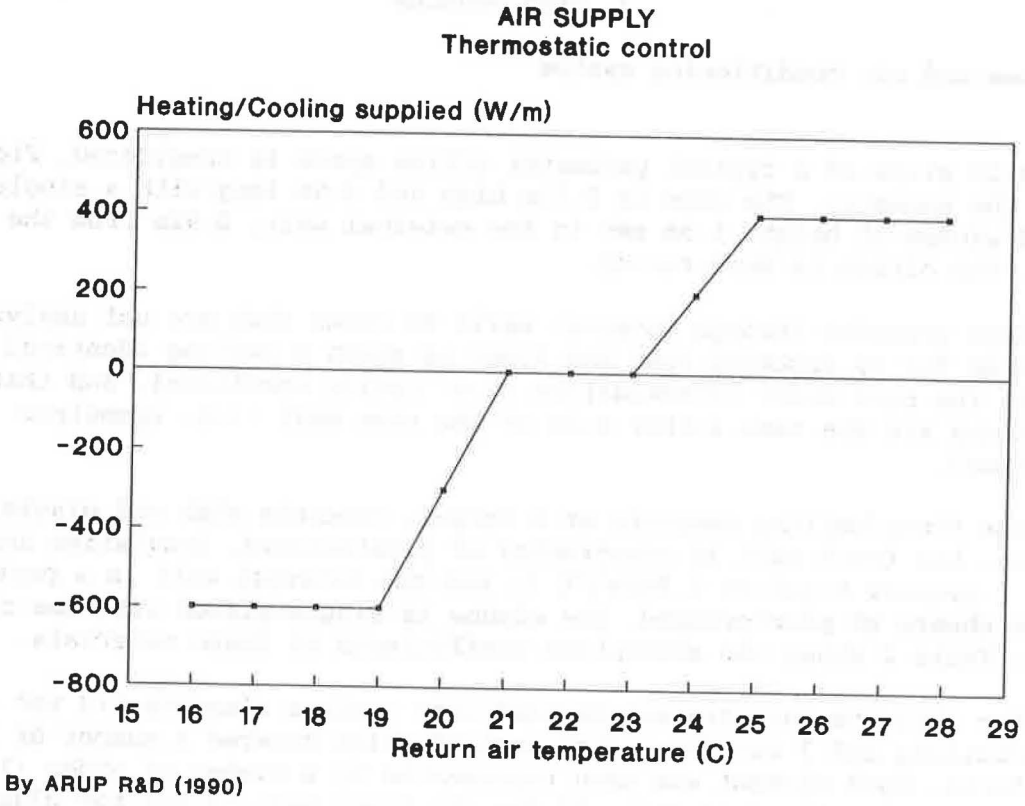

Fig. 2. Thermostatic control of air supply

AIRFLO, 1,200 cells were used to define the space, 40 in the horizontal direction and 30 vertically.

Table 2. Absorption coefficient

Surface	Absorption coefficient	
	long wave	short wave
Floor	0.90	0.6
Ceiling	0.85	0.6
Internal wall	0.85	0.6
External wall	0.85	0.6
Glazing	0.90	-

The room air distribution system consists of a linear slot diffuser located in the ceiling above the external wall and a return air grille positioned near the base of the opposite internal wall. Air is supplied at a constant volume flow rate of $0.022m^2/s$ giving a jet of momentum thickness 7.2mm. The temperature of the air supply is controlled by a sensor located at the return air grille. Figure 2 shows how the maximum supply air heating and cooling is varied as a function of return air temperature. The time constants of the sensor and heater battery are 15 seconds and 30 seconds, respectively, with a first-order differential equation being used to model response. Where R2D2 was operated alone (at a time-step of 30s) the response of the sensor and heater battery was considered instantaneous to avoid problems of instability.

Between 6pm and 8am the air supply is switched off.

3.2 External environment

Weather data giving details every 6 minutes of external air temperature, and direct solar and diffuse radiation was taken from a winter period of the CIBSE Example Weather Year (8).

4. SIMULATIONS

In order to evaluate the effect of using R2D2 and AIRFLO sequentially and with the fully coupled program, two simulations were performed:-

(A) R2D2 alone (ie. with a simple one-air-point model) until 10am using a time step of 30 seconds, and then AIRFLO in steady-state mode to determine the detailed air flow pattern (using thermal boundary conditions at 10am from R2D2).

(B) R2D2 alone until 9am, using a time-step of 30s, and then a fully coupled transient AIRFLO/R2D2 simulation until 10am (using a steady-state AIRFLO solution at 9am as an initial solution), at a time step of 1 second to ensure stability and good transient resolution.

Since the building fabric has a time constant of many hours R2D2 was

first operated for four days prior to the comparative simulations, to achieve realistic fabric temperatures. This was done, of course, with the simple one-air-point model. During this time the external air temperature varied between -6°C and +4°C.

Results are presented, below, for the period from 8am (when the air supply switches on) and 10am. During this time the external air temperature was between 0°C and 1°C and diffuse solar radiation varied between 10 and 200 W/m^2. No direct solar radiation was present since the room faces West.

5. RESULTS

5.1 Comparing sequential and coupled simulations

Figures 3.a) and 4.a) show the velocity fields for the two simulations. In both cases it can be seen that there is a cold down draught at the window, which would cause some local discomfort, and that the hot supply air does not circulate efficiently in the occupied zone. The two simulations produce remarkably similar air flow patterns.

Figures 3.b) and 4.b) show the temperature fields, which again have very similar forms but with dissimilar overall variations owing to the difference in supply air temperature (26°C when R2D2 is operated alone and 32°C from the coupled execution).

Figure 5. shows the supply air temperature, average surface temperature and average air temperature in the occupied zone (below a height of 1.8m) between 8am and 10am for the two simulations. The following effects can be seen:

Supply air temperature. In the fully coupled simulation the supply air temperature shows large oscillations. This is because of fluctuations in air temperature at the return air grille. This could be expected since the grille is sited in a region of relatively high temperature gradient where the cold downdraught meets the convective flow from the warm supply air (see Section 5.2). Such details are, by definition, not resolved when using the one-air-point simulation approach (ie. R2D2 being operated alone).

Average air temperature (occupied zone). A damped oscillation in the average air temperature lagged that of the supply air by a few minutes, principally because of the heat capacity (16.3kJ/kg/°C) and dynamics of the room air. The difference between the two simulations is, however, small in this respect since the air supply controller held the mean air temperature close to 20°C.

Average surface temperature. A slightly increased (<0.5°C) average surface temperature is seen for the fully coupled simulation. At 10am the glazing has an internal surface temperature of 7°C, while other surfaces are between 17°C and 20.5°C.

5.2 Oscillation of air movement pattern

From the behaviour of the supply air temperature in Figure 5., and the

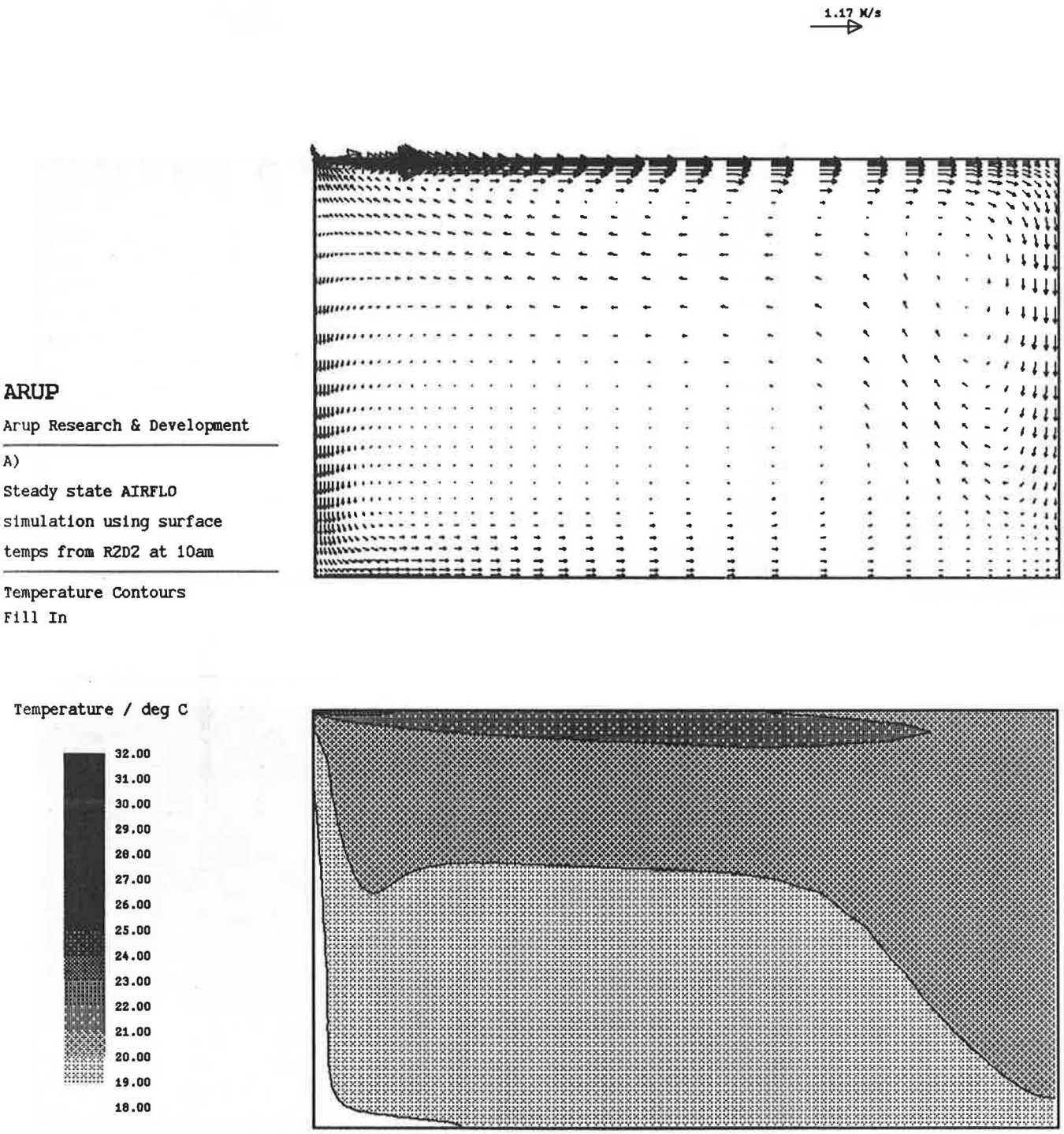

Fig. 3. Steady state AIRFLO simulation using surface temperatures from R2D2 at 10am.
a) Velocity field b) Temperature contours.

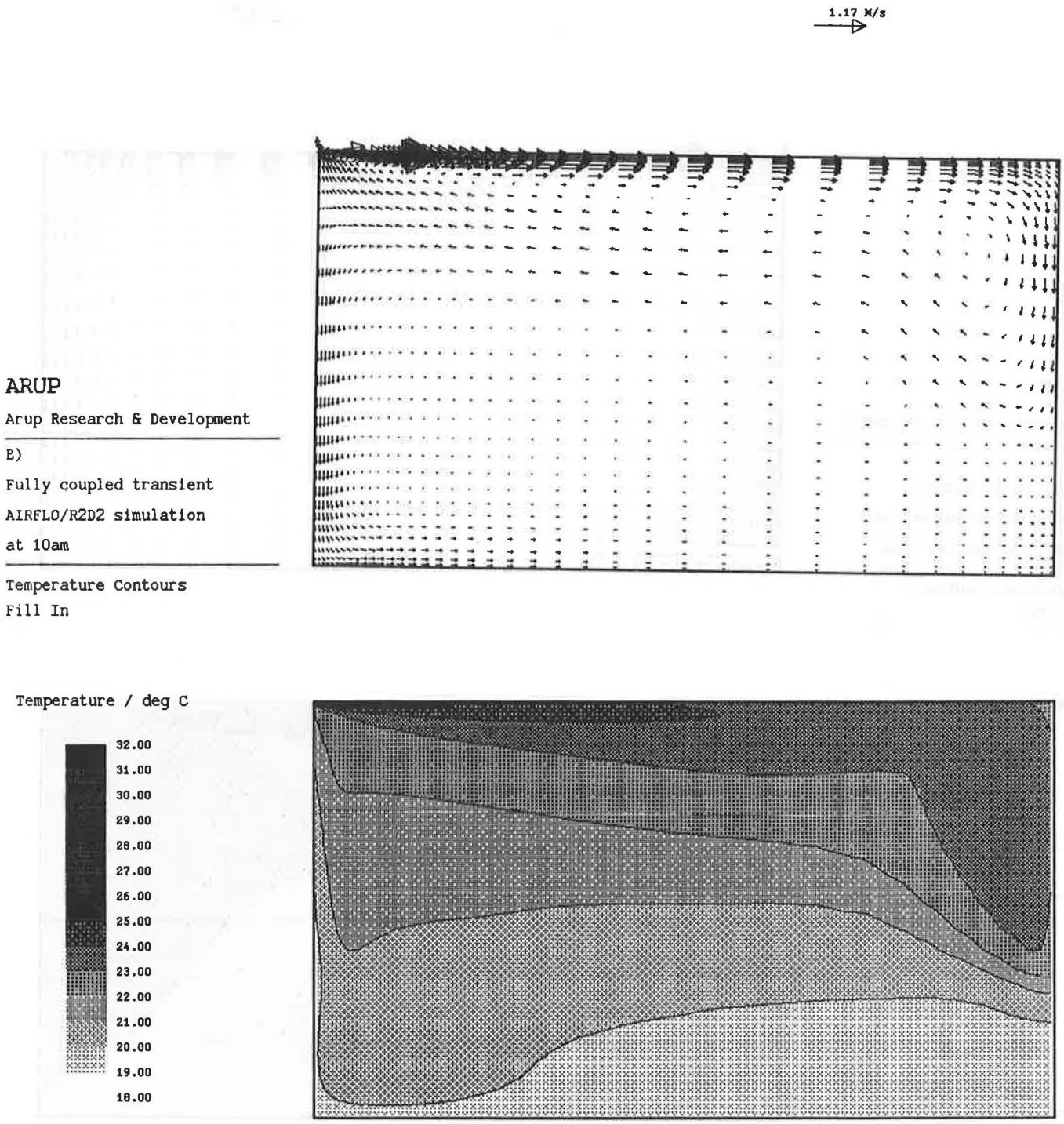

Fig. 4. Fully coupled transient AIRFLO/R2D2 simulation at 10am.
a) Velocity field b) Temperature contours.

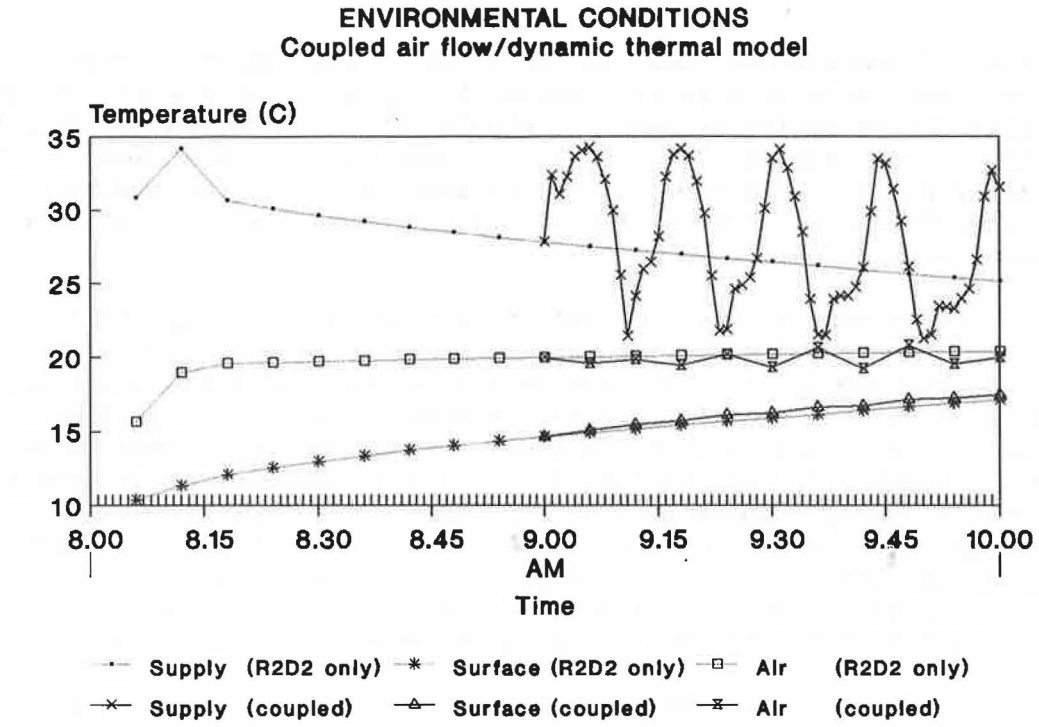

By ARUP R&D (1990)

Fig. 5. Environmental conditions - comparing simulations A) and B)

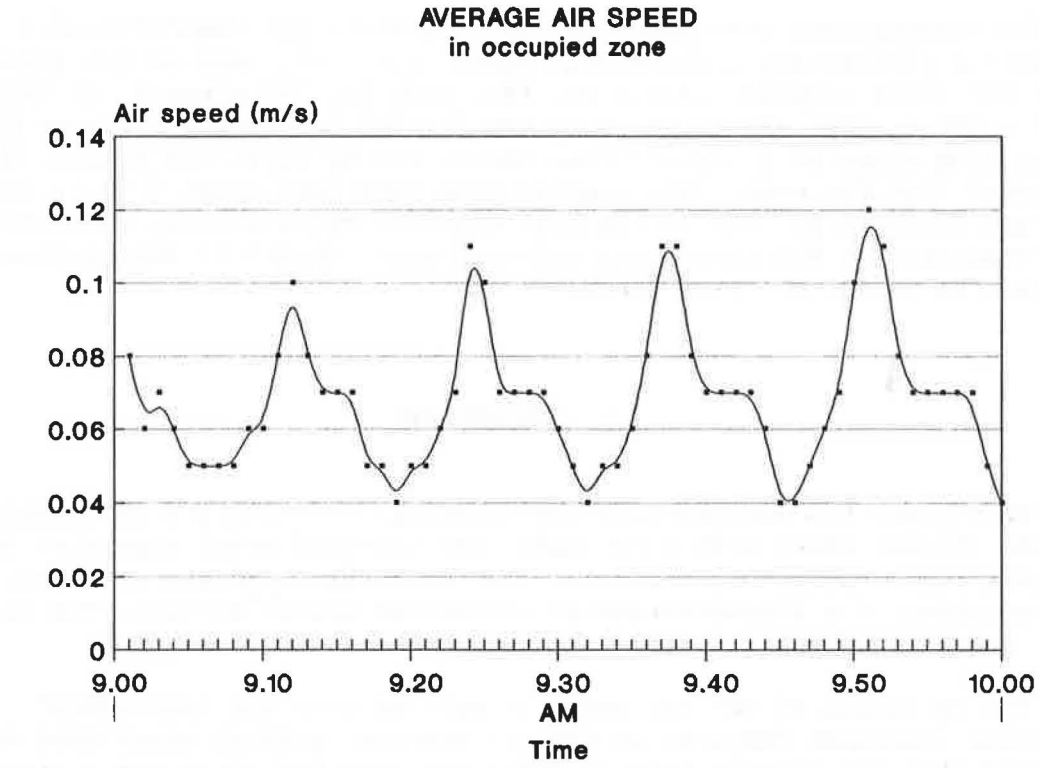

By ARUP R&D (1990)

Fig. 6. Average air speed in the occupied zone

variation of average air speed in the occupied zone shown in Figure 6. it is clear that there is a fairly regular and growing oscillation of the air flow with a time period of about 15 minutes. By considering the flow fields at times 9:50am (Figures 7.a) and b)), 9:54am (Figures 8.a) and b)) and 10:00am (Figures 4.a) and b)) it can be seen that this oscillation is associated with the nature of the air supply controller and the siting of the temperature sensor.

At one extreme of the oscillation (9:50am) air is supplied at relatively low temperature with respect to the room air and has little buoyancy. The supply air flow reaches the outlet (and temperature sensor) and runs along the floor for a distance before recirculating. This is, however, not a stable equilibrium since the air is losing heat to the cold surfaces. Eventually even the air at the outlet becomes cooler causing an increase in supply temperature. At the other extreme of motion the cold downdraught from the window runs along the floor reaching the outlet. In response, the temperature of the supply air is increased; and, although the warmer air doesn't, because of buoyancy force, directly reach the outlet it recirculates at a higher level raising the mean air temperature.

Since these two extreme air flow patterns are unstable the system oscillates between the two. This is a physical problem which would could be overcome by, for example, introducing a longer time delay on the air supply controller. Preliminary studies were made for a higher volume flow rate of $0.03m^2/s$ (and, hence, about double the supply momentum), which gave a well-mixed air-flow in the space with virtually no down-draught at the window, but a high average (and potentially uncomfortable) air speed of 0.3m/s. In this case no such oscillation of the system was observed.

5.3 Computation details

The computations were performed on an 8 Mbyte SUN SPARCstation-1. The sequential R2D2/steady state AIRFLO simulation, (A), took 22 CPU minutes, while the fully coupled simulation, (B), took 403 CPU minutes. Of this, about 2 CPU minutes was taken up by the initial four day phase when R2D2 was running alone at 30 second time steps, and by input and output. It is estimated that for each fully coupled time step only about 0.5% of the CPU time was taken up by R2D2 in the heat transfer calculations, with the run-time dominated by the heavy computational requirements of the transient CFD analysis at one-second time steps.

6. CONCLUSIONS

This paper has demonstrated the technical practicality of combining a dynamic thermal model with a CFD code. The combined model simulates long and short wave radiation, transient heat conduction and air movement, and the operation of a thermostatically controlled heater battery. The two codes are coupled via convective heat transfer at surfaces.

The operation of the two codes in coupled mode has highlighted important transient features of the air movement pattern which were not resolved when the dynamic thermal model was operated alone and a steady-state CFD analysis performed. Specifically, in this particular configuration of room an oscillation was evident of the air flow pattern in

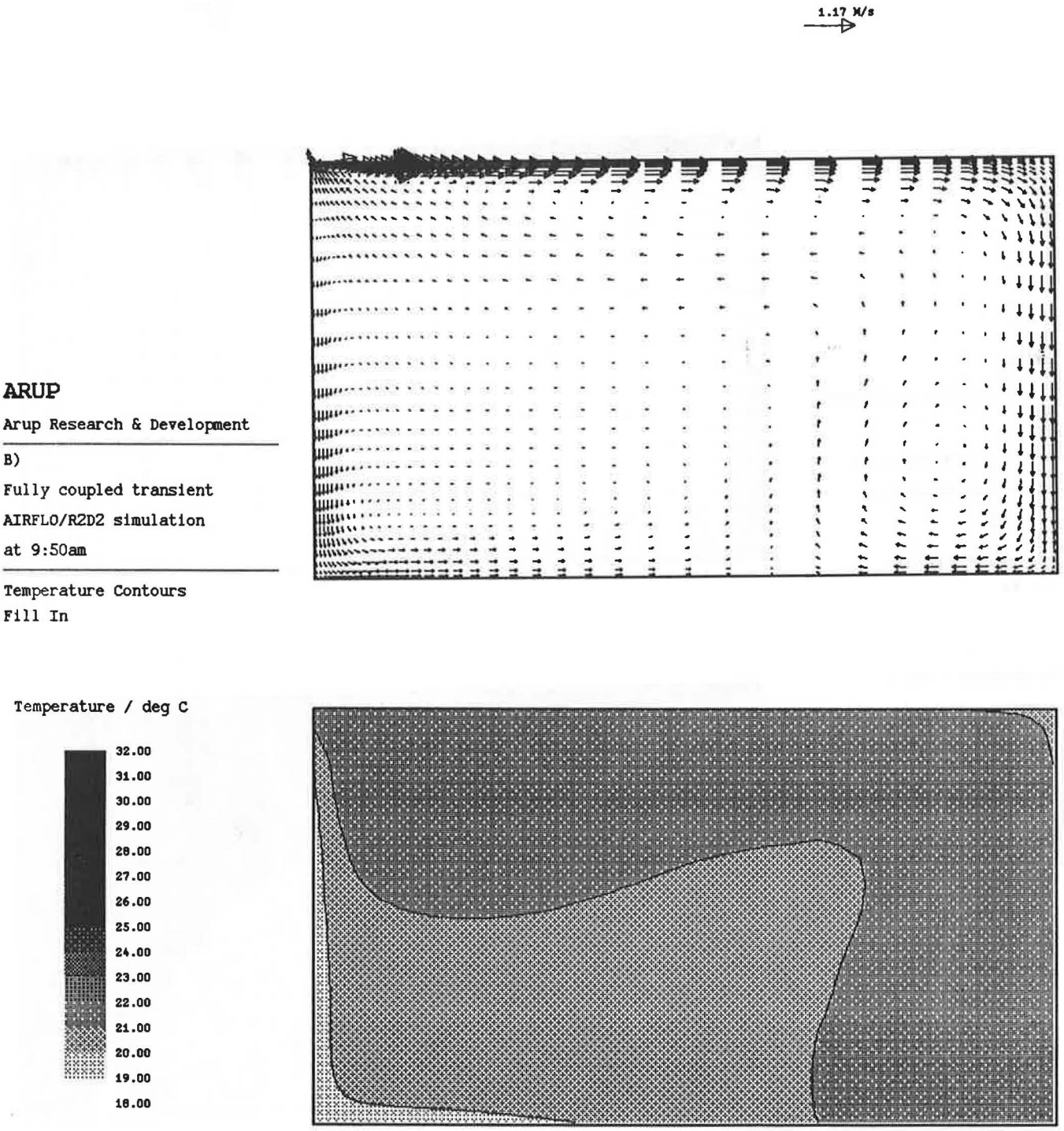

Fig. 7. Fully coupled transient AIRFLO/R2D2 simulation at 9:50am.
a) Velocity field b) Temperature contours.

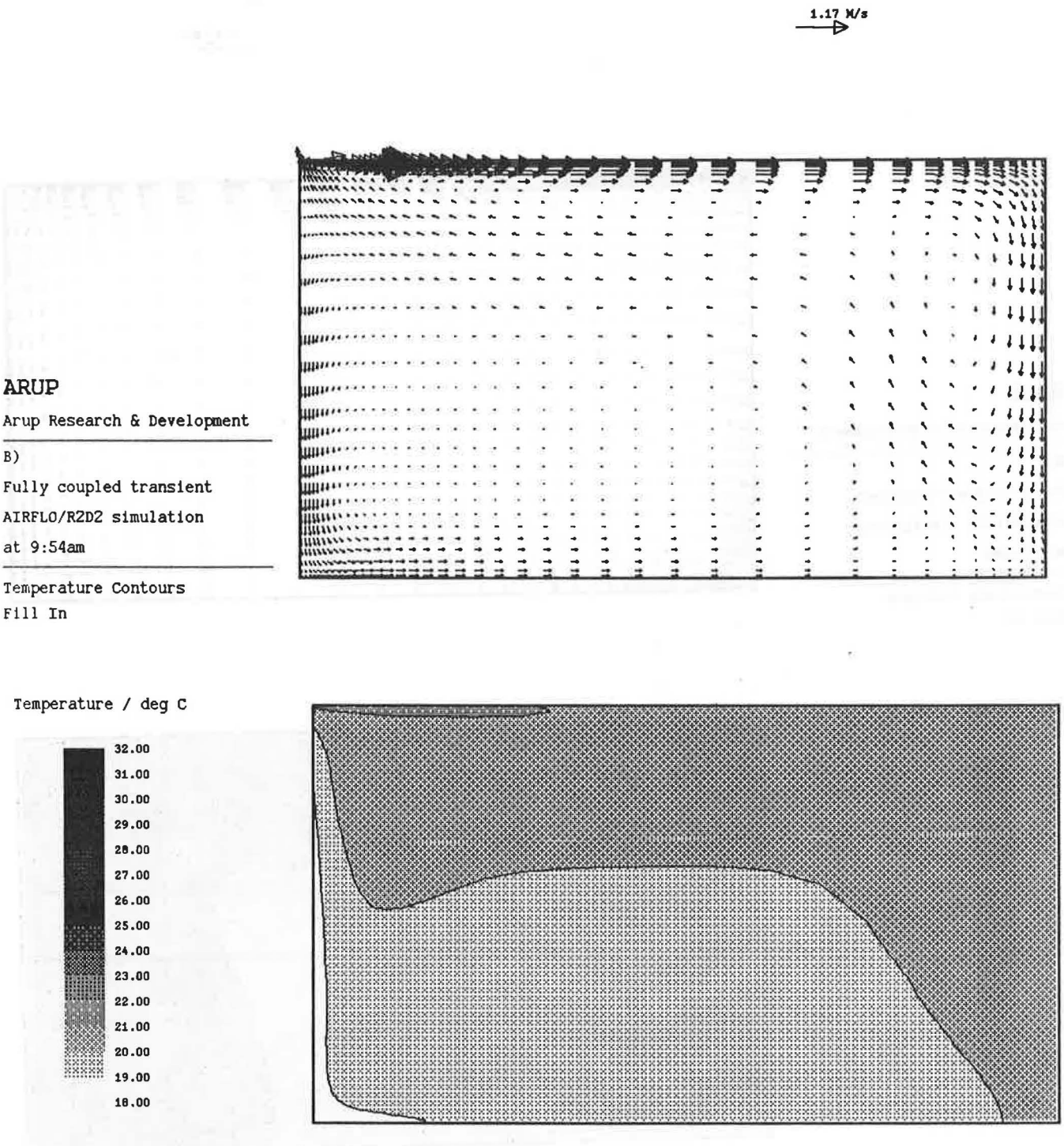

Fig. 8. Fully coupled transient AIRFLO/R2D2 simulation at 9:54am.
a) Velocity field b) Temperature contours.

the space. This, feature, which was due to a design weakness, would probably be overcome by increasing the time constant of the controller. Such phenomena could not be predicted by a dynamic thermal model using a fully mixed air flow approximation nor by a steady-state CFD simulation.

The fully-coupled operation of the models was found to be computationally very intensive, and so unless a detailed transient resolution (one-second time steps) is thought to be necessary then a significant reduction of total computational effort may be possible by extending the integration time step. Alternatively, a simpler analysis could be undertaken by operating the two codes sequentially and performing a steady-state CFD analysis at the time-frame when the most severe (design) conditions occur.

The overhead of operating the dynamic thermal model was found to be 0.5%. The run-time being dominated by the heavy computational requirements of the transient CFD analysis.

The arrangement of a ceiling-mounted diffuser discharging in a direction away from a cold single-glazed window was seen to produce a cold down draught and some evidence of discomfort.

Further work is necessary to refine the control action within this particular system configuration, and then, more generally, to identify the computational benefits and the penalties of extending the integration time step.

7. ACKNOWLEDGEMENT

The authors acknowledge the contribution of Sarah Dyke in preparation of the code for two dimensional form factors and internal solar distribution.

8. APPENDIX - Discretized CFD equations

Discretized momentum equation in X direction

$$a_P U_P = a_N U_N + a_S U_S + a_E U_E + a_W U_W + a_H U_H + a_L U_L + b_U$$

where
- a = convection / diffusion fluxes - a function of (C, D)
- C = convection (mass) flux
- D = diffusion flux
- $a_P = a_N + a_S + a_E + a_W + a_H + a_L + Vol.rho_P / dt$
- b_U = momentum source + $Vol.rho_P^{\circ}.U_P^{\circ} / dt$
- Vol = cell volume
- rho = density
- U = computed velocity
- U° = velocity at previous time step
- dt = time step

Subscript P refers to the in-cell variable value, and subscripts N, S, E, W, H and L refer to surrounding north, south, east, west, high and

low variable values. Superscript 'o' refers to the variable value at the previous time step.

The form of the function defining a_N, etc, follows from the selection of the discretization scheme, eg. upwind, central, hybrid differencing.

Discretized mass continuity equation

$$(rho_P - rho_P^o).Vol / dt + C_N + C_S + C_E + C_W + C_H + C_L + b_c = 0$$

where b_c = mass source

Discretized energy equation

$$a_P h_P = a_N h_N + a_S h_S + a_E h_E + a_W h_W + a_H h_H + a_L h_L + b_h$$

where h = enthalpy ($C_p T$)
C_p = specific heat
T = temperature
b_h = energy source + $Vol.rho_P^o.h_P^o / dt$

9. REFERENCES

(1) Alamdari,F., Hammond,G.P., and Mohammad,W.S. Computation of air flow and convective heat transfer within space-conditioned, rectangular enclosures. 5th International Symposium on the use of computers for environmental engineering related to buildings, Bath, England. July 1986.

(2) Moser,A. Trends in airflow design and management - contributions by IEA annex 20. 10th AIVC conference, Dipoli, Finland. September 1989.

(3) Holmes,M.J. Heat loss from Rooms: Comparison of determination methods. BSER&T 9(2), 69-78, (1988).

(4) Zedan,M., and Schneider,G.E. A coupled strongly implicit procedure for velocity and pressure computation in fluid flow problems. Numerical Heat Transfer, vol.8, pp.537-557, 1985.

(5) Patankar,S.V. Numerical heat transfer and fluid flow. Hemisphere Publishing Corporation, New York, 1980.

(6) Galpin,P.F., and Raithby,G.D. Treatment of non-linearities in the numerical solution of the incompressible Navier-Stokes equations. International Journal for Numerical Methods in Fluids, vol.6, pp.409-426, 1986.

(7) CIBSE guide. Practical data on heat transfer. pp.C3-12/13. CIBSE, London. 1986

(8) Hitchin,R., Holmes,M., Hutt,B., Irving,S., Nevrala,D. The CIBSE Example Weather Year, BSER&T, 4(3), 119-124, (1983).